

Tunneling Study of Superconductivity in Tl-Pb-Bi Alloys*

R. C. DYNES,† J. P. CARBOTTE, AND D. W. TAYLOR

Department of Physics, McMaster University, Hamilton, Ontario, Canada

AND

C. K. CAMPBELL

Institute for Materials Research, McMaster University, Hamilton, Ontario, Canada

(Received 8 July 1968)

Superconducting characteristics for selected alloys of the fcc Tl-Pb-Bi system have been measured using the technique of single-particle electron tunneling. Also, calculations of the electron-phonon coupling strength and hence the product function $\alpha^2(\omega)F(\omega)$ determining superconductivity in these alloys have been performed. The computations are based on neutron scattering data, an electron-ion pseudopotential form factor adjusted to fit experimental phonon dispersion curves, and a Born-von Kármán force-constant analysis. Through a solution of the Éliashberg gap equations, a critical comparison is made between the calculated $\alpha^2(\omega)F(\omega)$ and the experimentally determined tunneling curves. It is found that, even though fine details of the phonon-spectrum critical points do not always agree, the calculated superconducting energy gap Δ_0 is, in all cases, in good agreement with experiment. Where confidence is felt in the Born-von Kármán analysis, the location of the experimentally determined critical points is in excellent agreement with those calculated from inelastic neutron scattering data, while the relative strengths of these singularities show discrepancies attributed to the alloy nature of the material under study.

I. INTRODUCTION

MANY of the predictions of the Bardeen-Cooper-Schrieffer (BCS)¹ theory of superconductivity were substantiated subsequently in the early tunneling experiments of Giaever.² By this same technique, however, deviations from the BCS predicted single-particle tunneling density of states were observed³ and shortly thereafter correlated^{4,5} with Van Hove singularities in the phonon density of states $F(\omega)$ as revealed in the inelastic neutron scattering data.⁶

A generalized extension of the BCS theory had been put forward by Éliashberg⁷ in which he considered the details of the electron-phonon interaction in an approximation known⁸ to be accurate to order $(m/M)^{1/2}$, where m is the electron mass and M is the ion mass. This generalization resulted in an energy-dependent energy gap parameter $\Delta(\omega)$. Using a model $F(\omega)$ determined from inspection of the tunneling results for lead,⁹ Schrieffer, Scalapino, and Wilkins¹⁰ provided us with

an elegant explanation of these deviations from BCS in the strongly coupled superconductor via the Éliashberg gap equations. In their work, the electron-phonon coupling function $\alpha^2(\omega)$ entering the formula was treated as a variable parameter independent of ω and adjusted such that the energy gap $\Delta(\Delta_0) \equiv \Delta_0$ agreed with the experimentally measured value. McMillan and Rowell¹¹ extended this method in an iterative fashion resulting in an estimate of the product function $\alpha^2(\omega)F(\omega)$ and the effective electron-electron repulsion term $N(0)U_c$, which reproduced very accurately the experimentally measured tunneling characteristics. In this way they determined the normal state parameters controlling superconductivity in Pb and a number of other systems.¹²

Swihart, Scalapino, and Wada¹³ developed the first absolute estimate of the strength and form of this coupling function $\alpha^2(\omega)$ and found it not to be a constant, but greater in the longitudinal phonon region of $F(\omega)$ than in the transverse region. In lead, they found the ratio to be of the order of 2. Their computations were not very accurate, however, and in the end they found it necessary to make a final adjustment of $\alpha^2(\omega)$ to get agreement with the measured gap edge.

The purpose of this paper is to demonstrate that we are now in a position to determine much more accurately this function $\alpha^2(\omega)$, and hence the function determining the superconducting nature of the material $\alpha^2(\omega)F(\omega)$. This calculation requires a detailed knowledge of the electron-ion pseudopotential form factor $\langle \mathbf{k} + \mathbf{q} | w | \mathbf{k} \rangle$ and the nature of the phonons of the

* Research supported by the National Research Council of Canada.

† Present address: Bell Telephone Laboratories, Inc., Murray Hill, N. J.

¹ J. Bardeen, L. N. Cooper, and J. R. Schrieffer, *Phys. Rev.* **108**, 1175 (1957).

² I. Giaever, *Phys. Rev. Letters* **5**, 464 (1960).

³ I. Giaever, H. R. Hart, and K. Megerle, *Phys. Rev.* **126**, 941 (1962).

⁴ J. M. Rowell and L. Kopf, *Phys. Rev.* **137**, 907 (1965).

⁵ D. J. Scalapino and P. W. Anderson, *Phys. Rev.* **133**, A291 (1964).

⁶ B. N. Brockhouse, T. Arase, G. Caglioti, K. R. Rao, and A. D. B. Woods, *Phys. Rev.* **128**, 1099 (1962).

⁷ G. M. Éliashberg, *Zh. Eksperim. i Teor. Fiz.* **38**, 966 (1960) [English transl.: *Soviet Phys.—JETP* **11**, 696 (1960)].

⁸ A. B. Migdal, *Zh. Eksperim. i Teor. Fiz.* **34**, 1438 (1958) [English transl.: *Soviet Phys.—JETP* **7**, 996 (1958)].

⁹ J. M. Rowell, P. W. Anderson, and D. E. Thomas, *Phys. Rev. Letters* **10**, 334 (1963).

¹⁰ J. R. Schrieffer, D. J. Scalapino, and J. W. Wilkins, *Phys. Rev. Letters* **10**, 336 (1963).

¹¹ W. L. McMillan and J. M. Rowell, *Phys. Rev. Letters* **14**, 108 (1965).

¹² W. L. McMillan and J. M. Rowell, in *Superconductivity*, edited by R. D. Parks (Marcel Dekker, Inc., New York, 1969).

¹³ J. C. Swihart, D. J. Scalapino, and Y. Wada, *Phys. Rev. Letters* **14**, 106 (1965).

material. If both of these properties are reliably known, and there is reason to believe that band-structure effects are not large, one should obtain reasonable agreement between the calculated value of Δ_0 and that measured experimentally. In addition, we will show, through the solution of the Eliashberg gap equations, that the predictions of the single-particle tunneling density of states $N_T(\omega)$ are in quite good agreement with those experimentally measured. In particular, results will be presented for the Tl-Pb-Bi series which indicate that the tunneling method is a reliable technique for phonon spectroscopy and the location of critical points.

In Sec. II the Eliashberg gap equations which determine superconducting properties from $\alpha^2(\omega)F(\omega)$ and $N(0)U_c$ are specified. A discussion of the pseudopotential form factor used for the alloys and the calculation of $\alpha^2(\omega)F(\omega)$ is outlined in Sec. III. In Sec. IV the experimental aspects of this work are discussed where they differ from standard techniques, and in Sec. V the results of the calculations, experiments and comparisons are presented for the alloy system. The electron concentration is systematically varied from 3.2 to 4 electrons/atom and the effect of this change of concentration is observed in the coupling function $\alpha^2(\omega)$ and, even more important, in the superconducting energy gap $\Delta(\Delta_0)$.

II. GAP EQUATIONS

Using a self-consistent perturbative approach, the irreducible self-energy $\Sigma(\mathbf{k};\omega)$ can be expanded in terms of the fully dressed propagator $G(\mathbf{k};\omega)$, which, in turn, is related to $\Sigma(\mathbf{k};\omega)$ through Dyson's equation. Following Migdal's proof⁸ that it would be accurate to order $(m/M)^{1/2}$, Eliashberg retained only lowest order dressed Coulomb and dressed phonon contributions to $\Sigma(\mathbf{k};\omega)$. Following this self-consistent prescription, and after some fairly detailed manipulations,¹⁴ the resulting four-dimensional equations can be reduced to a pair of coupled, one-dimensional integral equations involving an energy-dependent gap function $\Delta(\omega)$ and a renormalization function $Z(\omega)$ of the form

$$\Delta(\omega) = \frac{1}{Z(\omega)} \int_{\Delta_0}^{\omega_c} d\omega' \operatorname{Re} \left(\frac{\Delta(\omega')}{[\omega'^2 - \Delta^2(\omega')]^{1/2}} \right) \times [K_+(\omega, \omega') - N(0)U_c], \quad (1a)$$

$$[1 - Z(\omega)]\omega = \int_{\Delta_0}^{\omega_c} d\omega' \operatorname{Re} \left(\frac{\omega'}{[\omega'^2 - \Delta^2(\omega')]^{1/2}} \right) \times [K_-(\omega, \omega')], \quad (1b)$$

where ω_c is a cutoff energy $\approx 10 \omega_{\text{Debye}}$ where the phonon contribution to $\Delta(\omega)$ has converged. Unfortunately, the electron-electron repulsion term has not converged at

¹⁴ J. R. Schrieffer, *Theory of Superconductivity* (W. A. Benjamin, Inc., New York, 1964).

ω_c and must be approximated by an effective repulsion term U_c given by¹⁵

$$U_c = V_c / [1 + N(0)V_c \ln(E_F/\omega_c)], \quad (2)$$

where E_F is the Fermi energy, V_c is the spherical average of the screened Coulomb potential between electrons, and $N(0)$ is the density of electron states at the Fermi surface. The kernels $K_{\pm}(\omega, \omega')$ in Eq. (1) are related to the contribution from the electron-phonon interaction to these equations and are defined by

$$K_{\pm}(\omega, \omega') = \int_0^{\infty} dv \sum_{\lambda} \alpha_{\lambda}^2(v) F_{\lambda}(v) \times \left(\frac{1}{\omega' + \omega + v + i0^+} \pm \frac{1}{\omega' - \omega + v - i0^+} \right), \quad (3)$$

where the product function¹⁶

$$\alpha_{\lambda}^2(v) F_{\lambda}(v) = \frac{1}{Nk_F} \int_{<2k_F} \frac{d^3q}{(2\pi)^3} \frac{m}{4M} \frac{|\mathbf{q} \cdot \boldsymbol{\varepsilon}(\mathbf{q}, \lambda)|^2}{|q|\omega(\mathbf{q}, \lambda)} \times |\langle (\mathbf{k} + \mathbf{q})_F | w | \mathbf{k}_F \rangle|^2 \delta(v - \omega(\mathbf{q}, \lambda)), \quad (4)$$

where $\boldsymbol{\varepsilon}(\mathbf{q}, \lambda)$ is the polarization of the $\omega(\mathbf{q}, \lambda)$ mode and λ is a branch index. The integral over momentum transfer $\mathbf{q} = \mathbf{k} - \mathbf{k}'$ is performed throughout a sphere of radius $2k_F$. This is determined by assuming a spherical Fermi surface and hence the maximum q transfer allowed is the diameter of the Fermi sphere. It is also assumed that the pseudopotential form factor $\langle (\mathbf{k} + \mathbf{q})_F | w | \mathbf{k}_F \rangle$ depends only on momentum transfer \mathbf{q} from one point on the Fermi surface to another (the local approximation). This assumption appears to be valid for the work reported here.

III. PSEUDOPOTENTIAL FORM FACTOR AND $\alpha^2(\omega)F(\omega)$

From Eq. (4) it is clear that in order to obtain a reliable estimate of the function $\alpha^2(\omega)F(\omega)$, it is first necessary to determine the form of the electron-ion pseudopotential form factor $\langle (\mathbf{k} + \mathbf{q})_F | w | \mathbf{k}_F \rangle$ or, in our approximation, $w(q)$.

This implies the use of a model whose parameters are to be determined from experimental data. Since we are particularly interested in the electron-phonon interaction, the model parameters are best obtained by fitting calculated phonon-dispersion relations to those obtained from the inelastic neutron scattering experiments.¹⁷ In fact there is no other source of information

¹⁵ N. N. Bogoliubov, V. V. Tolmachev, and D. V. Shirkov, *A New Method in the Theory of Superconductivity* (Consultants Bureau Enterprises, Inc., New York, 1959).

¹⁶ J. P. Carbotte and R. C. Dynes, *Phys. Rev.* **172**, 476 (1968).
¹⁷ B. N. Brockhouse, E. D. Hallman, and S. C. Ng, in *Magnetic and Inelastic Scattering of Neutrons by Metals*, edited by T. J. Rowland and P. A. Beck (Gordon and Breach, Science Publishers, Inc., New York, 1968).

TABLE I. Fitted parameters for $w(q)$ for $\text{Pb}_{0.4}\text{Tl}_{0.6}$ and $\text{Tl}_{0.3}\text{Bi}_{0.2}$.

Alloy	Parameters			
	A_0	A_1	A_2	β
$\text{Pb}_{0.4}\text{Tl}_{0.6}$	1.63	1.61	1.52	3.4
$\text{Tl}_{0.3}\text{Bi}_{0.2}$	1.61	1.61	1.52	3.4

to determine these parameters in the case of alloys. Since the only other information required in Eqs. (1) and (4) consists of these dispersion relations at a general wave vector, the procedure in this paper reduces to calculating the superconducting properties of a material solely from a knowledge of its phonon-dispersion relations along the symmetry directions.

Following the approximation made throughout this paper, the phonon calculations are performed as if the alloys were pure simple metals, yielding some sort of averaged electron-ion potential. The basic phonon calculation is then standard.¹⁸ The phonon frequencies and eigenvectors are obtained by solving

$$\omega^2(\mathbf{q}, \lambda) \varepsilon_{\alpha}(\mathbf{q}, \lambda) = \sum_{\beta} D_{\alpha\beta}(\mathbf{q}) \varepsilon_{\beta}(\mathbf{q}, \lambda), \quad (5)$$

where the dynamical matrix $D_{\alpha\beta}(\mathbf{q})$ is given by

$$D_{\alpha\beta}(\mathbf{q}) = \Omega_p^2 \sum_{\mathbf{K}_n} [(\mathbf{K}_n + \mathbf{q})_{\alpha} (\mathbf{K}_n + \mathbf{q})_{\beta} F(|\mathbf{K}_n + \mathbf{q}|) - (\mathbf{K}_n)_{\alpha} (\mathbf{K}_n)_{\beta} F(|\mathbf{K}_n|)]. \quad (6)$$

Here Ω_p^2 is the ion plasma frequency at $K=0$, and \mathbf{K}_n are the inverse lattice vectors.

The function $F(Q)$ is a sum of two terms. The first, $F_c(Q)$, describes the Coulomb interaction of the ions due to their valence charges Z , and is reduced (screened) by the second term $F_e(Q)$, which describes the interaction of the conduction electrons with these ions. The Coulomb term is simply

$$F_c(Q) = 1/Q^2. \quad (7)$$

$F_e(Q)$ depends upon the choice of model for the electron-ion potential and the nature of the approximation used in describing the interacting electron gas. We have based our choice of potential on that due to Heine and Abarenkov (HA)¹⁹ which has already been used with considerable success by Animalu *et al.*²⁰ in a first-principles calculation of phonon-dispersion relations. The model potential consists of a square well of radius $r=R_m$ and equals Z/r for $r > R_m$. Different well depths A_l are chosen for the scattering of different partial waves leading to a nonlocal potential. In the simple metals it is satisfactory to set the well depths equal for $l > 2$ so that three parameters, i.e., the three well depths A_0 , A_1 , and A_2 , describe this model. The parameters used by Animalu *et al.*²⁰ were those obtained by HA from fitting to free-ion data, whereas we have allowed them to be adjustable.

¹⁸ W. A. Harrison, *Pseudopotentials in the Theory of Metals* (W. A. Benjamin, Inc., New York, 1966).

¹⁹ V. Heine and I. Abarenkov, *Phil. Mag.* **9**, 451 (1964).

²⁰ A. O. E. Animalu, F. Bonsignori, and V. Bortolani, *Nuovo Cimento* **44B**, 159 (1966).

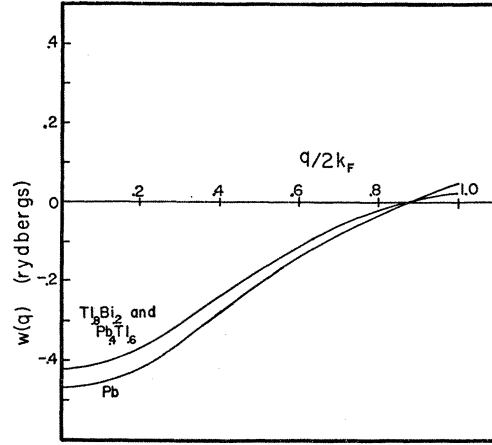


Fig. 1. Fitted forms of the electron-ion pseudopotential form factor $w(q)$ for $\text{Pb}_{0.4}\text{Tl}_{0.6}$, $\text{Tl}_{0.3}\text{Bi}_{0.2}$, and Pb.

Since we are fitting to experiment, no allowance has been made for the orthogonalization-hole correction. Shaw and Harrison²¹ have recently shown that the HA procedure is incorrect and unnecessary in the full non-local model when the energy dependence of the well depths is taken into account. We have also found that the HA correction gives a divergent contribution to the cohesive energy in our local approximation described below. Presumably, in our approximation an effective valence should have been used, as in orthogonal-plane-wave (OPW) calculations.

This bare model potential is screened by the electron gas and we have used the random-phase approximation (RPA) for the dielectric constant modified to take into account exchange corrections following a method suggested by Hubbard²² and employed by many authors. The simplest form of screening is used for the Coulomb interaction entering these corrections, i.e., Thomas-Fermi. Various suggestions have been made for the appropriate screening length to be used,^{23,24} but since

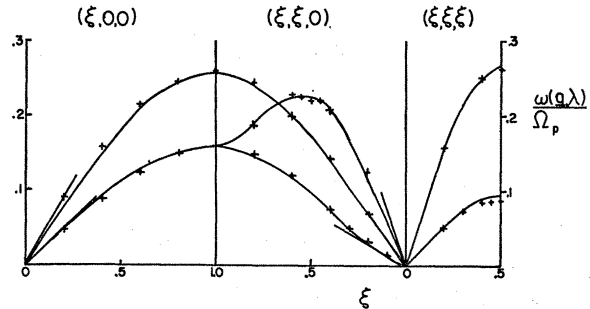


Fig. 2. Dispersion relations (lines) calculated from fitted pseudopotential compared with representative experimental points for $\text{Pb}_{0.4}\text{Tl}_{0.6}$ (+) (Ref. 17). The straight lines are the experimental sound velocities [See M. L. Shepard and J. F. Smith, *Acta Met.* **15**, 357 (1967)]. (Ω_p for this alloy is 5.8×10^{13} rad/sec.)

²¹ R. W. Shaw and W. A. Harrison, *Phys. Rev.* **163**, 604 (1967).

²² J. Hubbard, *Proc. Roy. Soc. (London)* **A244**, 199 (1958).

²³ V. Heine and L. M. Falicov, *Advan. Phys.* **10**, 57 (1961).

²⁴ D. J. W. Geldhart and S. H. Vosko, *Can. J. Phys.* **44**, 2137 (1966).

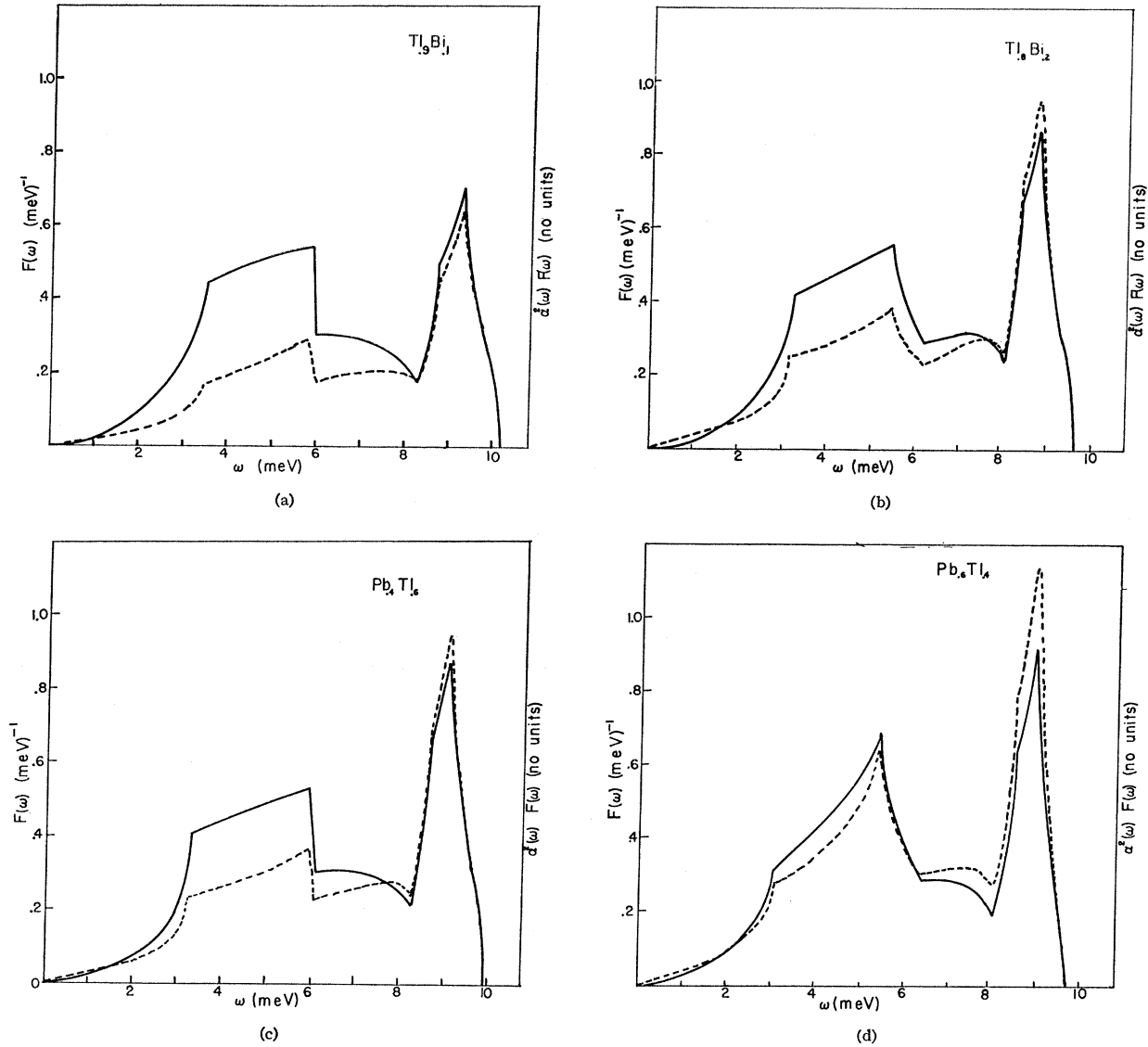


FIG. 3. Calculated $F(\omega)$ (solid line) and $\alpha^2(\omega)F(\omega)$ (dashed line) as a function of phonon energy ω for (a) $\text{Tl}_{0.9}\text{Bi}_{0.1}$, (b) $\text{Tl}_{0.8}\text{Bi}_{0.2}$, (c) $\text{Pb}_{0.4}\text{Tl}_{0.6}$, (d) $\text{Pb}_{0.6}\text{Tl}_{0.4}$, (e) $\text{Pb}_{0.8}\text{Tl}_{0.2}$, and (f) Pb .

the correction is only approximate, we have allowed this length to be an adjustable parameter. The use of a nonlocal potential throughout the calculation would require a prohibitive amount of computation time. It is possible to screen the nonlocal potential²⁵ and then make it local²⁰ but, since we are fitting, we have made the potential local before screening with a consequent further reduction in computation time.

As a result of these approximations,

$$F_\epsilon(Q) = -\frac{\epsilon(Q)-1}{\epsilon(Q)} \left(\frac{w'(Q)}{Q} \right)^2, \quad (8)$$

with

$$w'(Q) = (\Omega Q^2 / 8\pi Z) w_{\text{HA}}(Q). \quad (9)$$

All the quantities on the right-hand side of Eq. (9) are in atomic units with Ω equal to the atomic volume and $w_{\text{HA}}(Q)$ is as given in the Appendix of Ref. 26. The dielectric constant $\epsilon(Q)$ is related to the RPA susceptibility $\pi_{\text{RPA}}(Q)$ by

$$\epsilon(Q) = 1 + \frac{v(Q)\pi_{\text{RPA}}(Q)}{1 - v(Q)f(Q)\pi_{\text{RPA}}(Q)}, \quad (10)$$

with

$$v(Q) = 4\pi e^2 / Q^2 \quad (11)$$

and

$$f(Q) = \frac{1}{2} Q^2 / (Q^2 + \beta^2), \quad (12)$$

where β is a measure of the inverse screening length used in the Hubbard correction.

²⁵ A. O. E. Animalu, *Phil. Mag.* **11**, 379 (1965).

²⁶ A. O. E. Animalu and V. Heine, *Phil. Mag.* **12**, 1249 (1965).

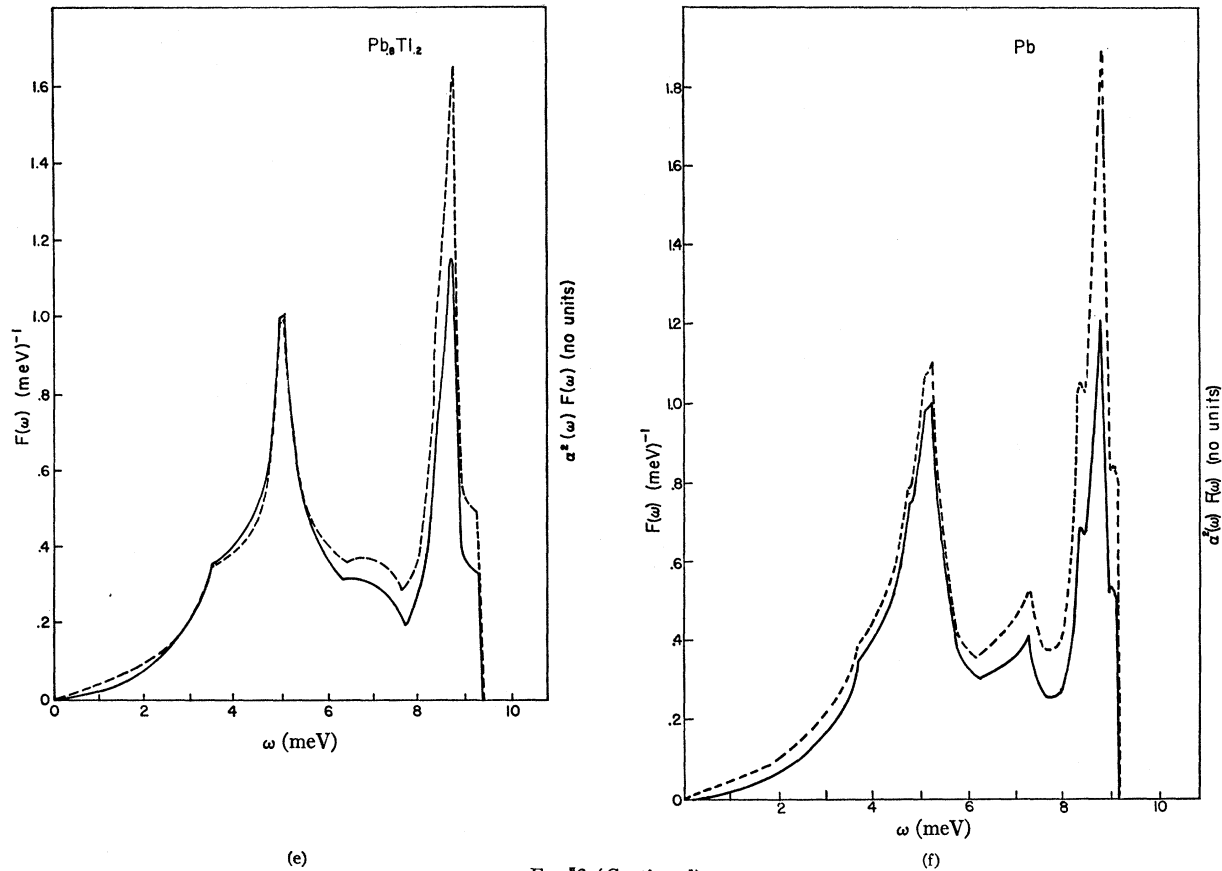


FIG. 3 (Continued)

Due to the unphysical discontinuity in the model potential at the edge of the well, $F_e(Q)$ oscillates. Convergence problems have been avoided by arbitrarily setting the potential $w_{\text{HA}}(Q)$ equal to zero beyond its second zero. Summing to the third zero gives only small shifts in those cases checked, and the cutoff appears to produce no structure in the dispersion relations. The Coulomb part of Eq. (6) is handled by the usual Ewald technique.

Because we were originally interested in using the model potential to calculate both the phonon frequencies and the electron-phonon interaction the parameters A_0 , A_1 , A_2 , and β were adjusted to give reasonable fits to the experimental frequencies at $(1,0,0)$ and $(\frac{1}{2}, \frac{1}{2}, \frac{1}{2})$. A trial-and-error method was used starting from the values suggested by HA and no uniqueness is claimed. We note that the frequencies are particularly sensitive to A_1 , and variations in β have their largest effect upon the longitudinal modes.

A more detailed discussion of the effects of variations of these parameters will be given elsewhere along with the application of the method to other materials.

The above procedure has been used for those alloys with $Z=3.4$ as good fits are then possible due to the electron-phonon interaction not being too strong. Fitted parameters are given in Table I, the potentials

are shown in Fig. 1, and a calculated dispersion relation is compared with experiment in Fig. 2. The fitted value of β is in close agreement with that suggested by Geldhart and Vosko.²⁴ To obtain form factors suitable for the remaining alloys, an interpolation scheme between our determined form factors and those published²⁶ for lead was employed.

In order to determine $\alpha^2(\omega)F(\omega)$, in addition to a knowledge of $w(q)$, a fairly detailed description of the phonons of that material is required. Since the pseudopotential method is a rather lengthy procedure from a computational point of view, and since a Born-von Kármán force-constant analysis is available¹⁷ and supplies us at this stage with a better fit to the symmetry direction dispersion curves, this type of description of the phonons is used. By adjusting empirical force constants between ions such that one can reproduce accurately all the available data in the symmetry directions, it is hoped that the method can be interpolated to off-symmetry points and the characteristics of the phonons $[\omega(\mathbf{q},\lambda)$ and $\mathbf{e}(\mathbf{q},\lambda)]$ for any given arbitrary \mathbf{q} vector can be determined. The lattice dynamics are then completely specified for the material, the accuracy of which is determined by the accuracy of the force-constant analysis.

To calculate $\alpha^2(\omega)F(\omega)$ we use a simple modification of the Gilat-Raubenheimer²⁷ computer program which was designed to determine $F(\omega)$ from a given set of force constants. While the calculation of $F(\omega)$ restricts itself to the irreducible 1/48 of the Brillouin zone in a cubic system, the present calculations must be extended to include the entire volume of a sphere of radius $2k_F$. Because of the translational and rotational symmetry of the cubic group, this extension is most easily effected by a systematic series of coordinate transformations generating from an original point on the 1/48. The force-constant model, which reduces to a 3×3 eigenvalue problem for these simple materials, conveniently furnishes us with both the eigenvalues $[\omega(\mathbf{q},\lambda)]$ and the eigenvectors $[\boldsymbol{\epsilon}(\mathbf{q},\lambda)]$ for any given \mathbf{q} .

From Eq. (4) it is now clear that we have all that is necessary to determine the product function $\alpha^2(\omega)F(\omega)$. Because of the $|\mathbf{q} \cdot \boldsymbol{\epsilon}(\mathbf{q},\lambda)|^2$ term, the integration throughout the first Brillouin zone is not expected to yield much of a contribution from the transverse phonons, and it is not until umklapp processes are allowed (\mathbf{q} extends out beyond the first Brillouin zone) that the lower-energy transverse phonons will make any significant contribution to $\alpha^2(\omega)F(\omega)$. For this reason, we would expect the function $\alpha^2(\omega)$ to be lower in the transverse region of $F(\omega)$ than in the longitudinal region, and the ratios of these values would be some sort of a measure of the umklapp processes considered. This difference in α_t^2 and α_l^2 was first pointed out by Scalapino, Wada, and Swihart,²⁸ and for lead it was found that

$$\alpha_t^2/\alpha_l^2 = 0.53.$$

The calculations of $\alpha^2(\omega)F(\omega)$ reported in the present work are only as accurate as the force-constant model used to calculate them. It has been pointed out recently²⁹ that the resultant $F(\omega)$ and $\alpha^2(\omega)F(\omega)$ calculated for lead using an eight-nearest-neighbor force-constant model show discrepancies with the tunneling data which can best be attributed to the nonconvergence of the force-constant model. This conclusion, as can be seen in the results reported here, can be extended to the alloys with high lead concentration. On the other hand, bulk properties depending upon integrals over these functions (such as specific heat, resistivity,³⁰ and Δ_0 ¹⁶) do not appear to depend critically on the fine structure.

The calculated $\alpha^2(\omega)F(\omega)$ superimposed on a normalized $F(\omega)$ for the six materials considered are illustrated in Fig. 3. As electron concentration increases, we see the strength of this product function increasing which is simply an increase in the electron-phonon coupling

strength $\alpha^2(\omega)$. Also, it should be noted that the function $\alpha^2(\omega)$ is less in the transverse energy region than in the longitudinal peak region. In fact, within the free-electron-model assumptions used, this function diverges for low ω as $1/\omega$. The reason for this has been discussed previously.¹⁶ On the other hand, when the band structure is included this low-energy behavior is modified. Consider a scattering from an initial to a final state on the Fermi surface with both states near zone boundaries corresponding to a small reduced momentum transfer and consequently small ω . The multi-OPW matrix elements necessary to describe such processes can be considerably different from a single-OPW¹⁸ leading to modifications at low ω . For pure Pb, McMillan and Rowell¹¹ assign the weak structure that they observed in tunneling experiments at 1.6 and 3.0 meV to such effects. It is not clear to us, however, that such considerations apply to alloys where scattering is rapid and where the energy becomes uncertain. In any case, we ignore such complications here. They are not expected to lead to large effects. Within the limitations of our model no new structure is resolved in $\alpha^2(\omega)$ and, consequently, the critical points observed in a tunneling experiment can be assumed to correlate with Van Hove singularities in $F(\omega)$. This assumption appears to be valid to a good approximation for the alloys considered.

IV. EXPERIMENTAL ASPECTS

The experiments reported here were performed on thin-film evaporated junctions of the aluminum-insulator-alloy configuration where plots were taken with both materials first in the superconducting state, and then in the normal state. Early alloy films were constructed by evaporating the previously prepared bulk alloy from a resistive heated molybdenum boat relying on the fact that, because the vapor pressures of the constituents of the alloys were approximately equal, the film concentrations would be homogeneous and the same as that of the bulk. This approach, for high thallium concentrations, yielded ambiguous results which could best be described as multiple gap behavior. These energy gaps appeared at different critical temperatures and were attributed to inhomogeneity of the concentrations throughout the film and possibly an ordering phenomenon. For this reason, we reverted to a flash evaporation technique which consisted of dropping small pellets (equivalent to, on the average, about 20 Å of film) of the alloy onto the resistive heated boat which was maintained at a temperature well above the vapor temperature of either component at 5×10^{-6} Torr. In this way it was hoped that any inhomogeneities in the alloy film would be extremely short range. Using this technique, no multiple gap behavior appeared. The alloy films were approximately 1000 Å thick.

Concentrations of the constituents of the alloy film were determined on an electron microprobe after the tunneling measurements were performed. It was found

²⁷ G. Gilat and L. J. Raubenheimer, Phys. Rev. 144, 390 (1966).

²⁸ D. J. Scalapino, Y. Wada, and J. C. Swihart, Phys. Rev. Letters 14, 102 (1965).

²⁹ R. C. Dynes, J. P. Carbotte, and E. J. Woll, Jr., Solid State Commun. 6, 101 (1968).

³⁰ J. P. Carbotte and R. C. Dynes, Phys. Letters 25A, 532 (1967).

that, averaged over the thickness of the film, the constituents were measured to be within $\pm 2\%$ of the concentrations of the bulk alloy.

The tunneling characteristics were measured in the standard fashion in order to get a value of the energy gap Δ_0 and the derivatives of these characteristics were determined using the harmonic detection technique. The value $\Delta_1 + \Delta_2$ was interpreted as the point of maximum slope on the $I-V$ characteristic while the point of zero slope on the low-energy cusp was assigned the value $\Delta_1 - \Delta_2$. For plots of dI/dV versus V , a modulating 1-kc/sec signal of amplitude $\approx 50 \mu\text{V}$ peak-to-peak was used, while to determine d^2I/dV^2 , it was found necessary to increase the signal to approximately $200 \mu\text{V}$ in order to extract any useful information. This increase did not appear to significantly alter the results.

Tunneling theory applied to nonsymmetric junctions tells us that in the configuration (superconductor a)-(insulator)-(superconductor b) at $T=0^\circ\text{K}$ the current is proportional to¹⁴

$$I(V) \propto \int_0^{eV} N_T^a(\omega) N_T^b(eV - \omega) d\omega,$$

where $N_T^a(\omega)$ refers to superconductor a and is the single-particle tunneling density of states written as

$$N_T(\omega) = \text{Re} \left(\frac{\omega}{(\omega^2 - \Delta^2(\omega))^{1/2}} \right).$$

Note that this is symmetric about $\omega=0$ (the Fermi level). To extend this tunneling relationship to finite temperatures simply requires a modification of these terms by the appropriate Fermi distribution functions

$$f(\omega) - f(\omega - eV),$$

and an extension of the upper limit of integration beyond the region where these functions are finite. Since aluminum was employed as one of the superconductors, and since the experiments were performed at 1.1°K , just slightly below the critical temperature T_c for aluminum, this finite temperature extension was considered in the analysis.

If the forms of $N_T^a(\omega)$ and $N_T^b(\omega)$ are known, then one is able to predict absolutely the normalized conductance

$$\sigma = \left(\frac{dI}{dV} \right)_s \left| \left(\frac{dI}{dV} \right)_n \right. \text{ versus } V$$

and its derivative

$$d\sigma/dV \text{ versus } V,$$

where s refers to the case where both materials are in the superconducting state, and n is the corresponding plot in the normal state. From a solution of the gap equations for a previously determined $\alpha^2(\omega)F(\omega)$ for alumi-

TABLE II. Calculated and measured values of the superconducting gap edge Δ_0 .

Material	No. of electrons/atom	$N(0)U_c$	Δ_0 calc. (meV)	Δ_0 expt. (meV)
Pb	4	0.13	1.49	1.38 ± 0.05
Pb _{0.8} Tl _{0.2}	3.8	0.12	1.37	1.27 ± 0.10
Pb _{0.6} Tl _{0.4}	3.6	0.12	1.08	1.02 ± 0.10
Pb _{0.4} Tl _{0.6}	3.4	0.10	0.67	0.68 ± 0.10
Tl _{0.8} Bi _{0.2}	3.4	0.10	0.67	0.66 ± 0.10
Tl _{0.9} Bi _{0.1}	3.2	0.10	0.38	0.35 ± 0.05

num,¹⁶ and from the work of other investigators,³¹ it was found that the maximum deviation from BCS predictions in $N_T(\omega)$ for aluminum is $\lesssim 0.02\%$. Also, this maximum deviation is in the region $\omega \approx 36 \text{ meV}$, well beyond the maximum phonon energy of the alloys considered. For these reasons, a finite temperature BCS $N_T(\omega)$ was assumed for aluminum.

When convenient, the normal-state studies were achieved by heating the sample above the transition temperature of either material, but for other concentrations it was found to be more convenient to apply a magnetic field to the device to drive it into the normal state.

V. RESULTS AND COMPARISONS

Tunneling experiments were performed on the materials Pb, Pb_{0.2}Tl_{0.8}, Pb_{0.6}Tl_{0.4}, Pb_{0.4}Tl_{0.6}, Tl_{0.8}Bi_{0.2}, and Tl_{0.9}Bi_{0.1} for which the $\alpha^2(\omega)F(\omega)$ parameters were calculated and the related energy gaps were measured from the resulting current-voltage characteristics. Theoretical values for the energy gaps of such alloys were also obtained from the solution of the Éliashberg gap equations for the appropriate $\alpha^2(\omega)F(\omega)$, and a comparison of the results obtained by the two methods is given in Table II. The errors quoted for the experimentally determined values include both instrumental measuring errors, and such errors, arising from preparation problems, as might be associated with uncertainties in the constituents of the alloys. Each experimentally measured value quoted represents at least two separate samples independently prepared in order to ascertain consistency.

The values of $N(0)U_c$ employed in Table II have been determined from a range of sources: calculated from Eq. (2), from the work of McMillan and Rowell,¹² and from the estimates of Wu.³²

From this comparison, it is clear that good agreement is achieved between that value observed and that calculated, particularly considering that no correction is introduced for the band-structure density of states at the Fermi surface. The evidence is that in Pb this should

³¹ S. B. Woods and J. S. Rogers, in *Proceedings of the Tenth International Conference on Low-Temperature Physics*, Moscow, 1966, edited by M. P. Malkov (*Proizvodstvenno-Izdatel'skii Kombinat, VINITI, Moscow, 1967*).

³² T. M. Wu, *Phys. Rev. Letters* **19**, 508 (1967).

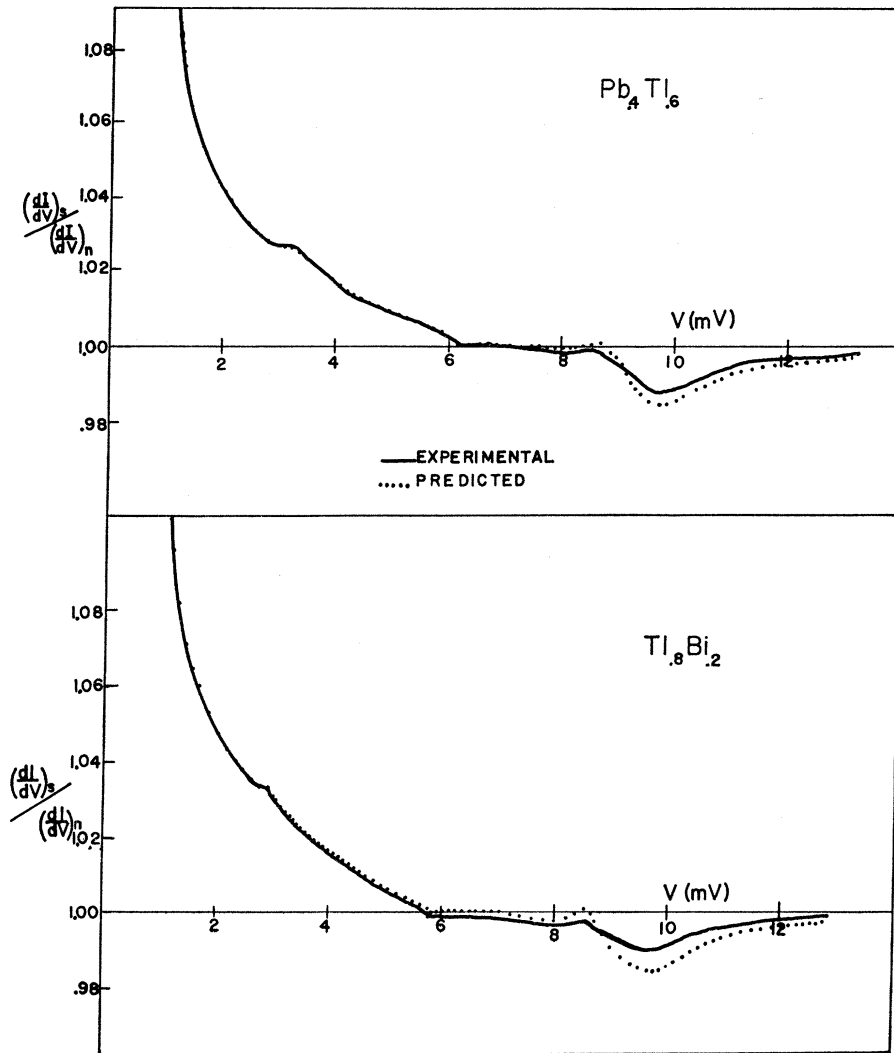


FIG. 4. Comparison of calculated (dotted line) and experimental (solid line) $(dI/dV)_s / (dI/dV)_n$ versus V plots for Al-I-Pb_{0.4}Tl_{0.6} and Al-I-Tl_{0.8}Bi_{0.2} junctions at 1.1°K.

be less than the free-electron value by about 10%. It is for this reason that we employed 0.13 for $N(0)U_c$ in Pb instead of the measured value of 0.12. It seems to us more consistent in the present context since $\alpha^2(\omega)F(\omega)$ is also directly proportional to $N(0)$. It should be pointed out that the two materials Pb_{0.4}Tl_{0.6} and Tl_{0.8}Bi_{0.2}, possessing the same electron concentrations (3.4 electrons/atom) and consequently very similar-sized Fermi surfaces, also display very similar superconducting properties. This result is not surprising, since we see from Fig. 3 that the functions $\alpha^2(\omega)F(\omega)$ for the two materials are almost identical, and as we shall see, the tunneling characteristics substantiate this.

From this analysis, the profound effect of electron concentration, and hence the size of the Fermi surface, on the coupling of electrons to phonons and on the onset of superconductivity becomes clearer.

By comparing calculated and experimentally determined values of the energy gap $\Delta(\Delta_0)$, we are comparing

bulk properties of these materials. There is, however, an even more critical comparison available when a tunneling experiment is performed on such a material. From the results of a tunneling experiment we can obtain a measure of the tunneling density of states $N_T(\omega)$. It is now clearly understood¹⁰ that deviations and critical points in this experimentally determined function are direct reflections of critical points in the product function $\alpha^2(\omega)F(\omega)$. Hence, assuming no effects due to band structure, $F(\omega)$ will have the same critical points as $\alpha^2(\omega)F(\omega)$ and, in turn, these same points will be reflected in the function $N_T(\omega)$.

With this in mind we first consider those particular alloys that display a reliable and converging force-constant model. The most reliable of the alloys considered in this respect were the two alloys having electron concentrations 3.4/atom, i.e., Pb_{0.4}Tl_{0.6} and Tl_{0.8}Bi_{0.2}. In order to compare calculated tunneling characteristics with those of experiment, the calculated

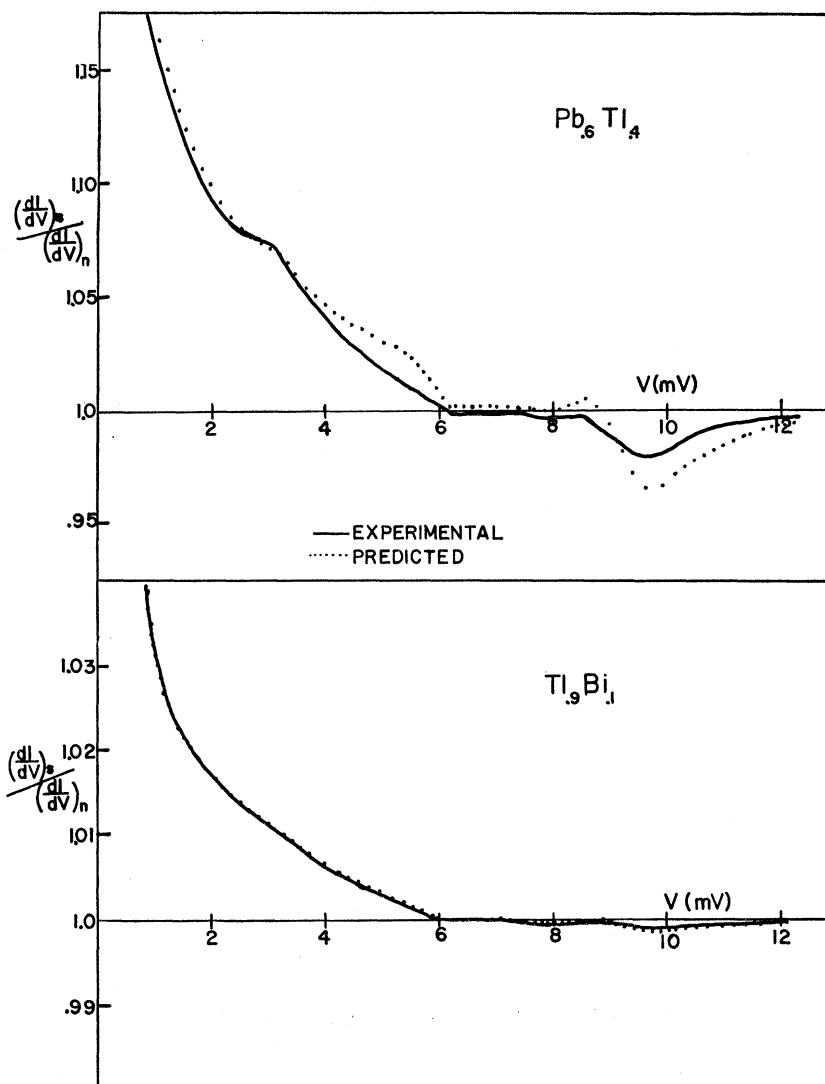


FIG. 5. Comparison of calculated (dotted line) and experimental (solid line) $(dI/dV)_s/(dI/dV)_n$ versus V plots for Al-I- $Pb_{0.6}Tl_{0.4}$ and Al-I- $Tl_{0.9}Bi_{0.1}$ junctions at 1.1°K.

$N_T(\omega)$ parameter for each alloy was convoluted with a BCS $N_T(\omega)$ with thermal excitations at 1.1°K representing the aluminum on the other side of the junction. The results of such a comparison with the normalized results of a tunneling experiment for those two particular alloys are shown in Fig. 4. The agreement between that predicted and the actual results of experiment is striking. It should also be recalled that excellent agreement was obtained with these particular alloys for the calculation of Δ_0 .

The procedure was repeated for alloys with a slightly less reliable force-constant fit, namely, $Pb_{0.6}Tl_{0.4}$ and $Tl_{0.9}Bi_{0.1}$, and the results are given in Fig. 5. As expected, there is more disagreement in these comparisons but, nevertheless, the over-all agreement is still acceptable. Even poorer agreement is expected with the other alloys because the force-constant model is even less reliable.

An even more critical comparison is that of comparing calculated and experimentally obtained plots of $d\sigma/dV$ versus V . Critical points in $N_T(\omega)$ are greatly amplified as a result of further differentiation.

In order to first determine the degree of agreement that could be expected in such a comparison, the $\alpha^2(\omega)F(\omega)$ for lead as determined by McMillan and Rowell¹² was treated in exactly the same fashion, convoluted with a 1.1°K BCS $N_T(\omega)$ for aluminum and $d\sigma/dV$ was determined. The comparison of this calculation and the experimental results of an Al-I-Pb junction is illustrated in Fig. 6. This determination was performed with a view to applying a circular consistency check which would serve as a standard for comparison.

With these factors in mind, $d\sigma/dV$ was determined for an Al-I-alloy junction at 1.1°K employing a grid in $\alpha^2(\omega)F(\omega)$ indicative of the ac sensing signal experimentally applied to the device. The results of this com-

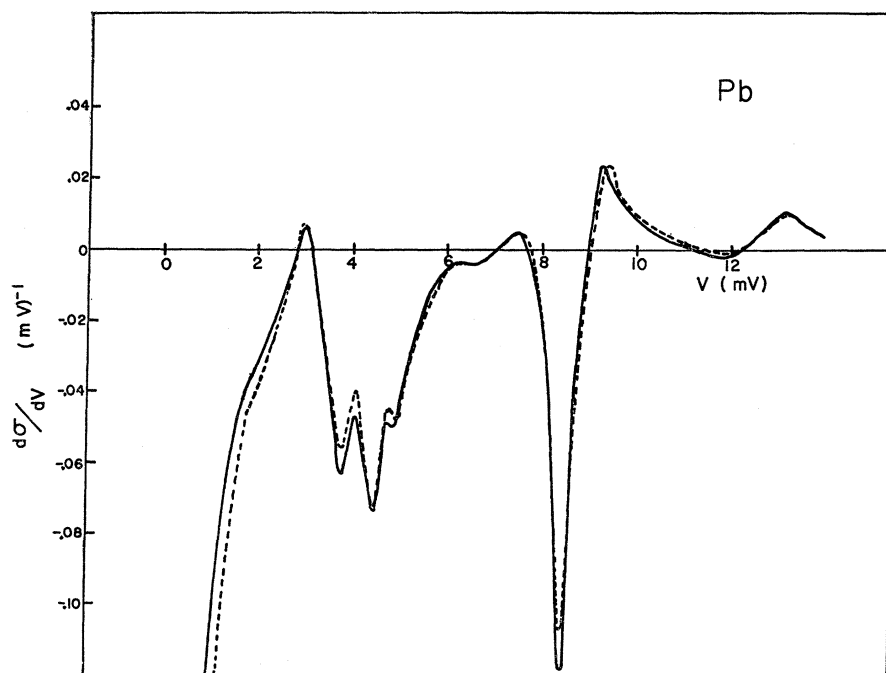


FIG. 6. A comparison of experimental (solid line) and calculated (dashed line) $d\sigma/dV$ versus V plots for an Al-I-Pb junction at 1.1°K. The $\alpha^2(\omega)F(\omega)$ used is that of McMillan and Rowell (Ref. 12).

parison for $Tl_{0.8}Bi_{0.2}$ and $Pb_{0.4}Tl_{0.6}$ are illustrated in Fig. 7. Excellent agreement in the positions of the critical points in energy is achieved, while in some regions, particularly the longitudinal range, discrepancies appear in the strengths of these peaks

For purposes of completeness, the remaining alloys considered are presented in Fig. 8 in this same fashion; one can see clearly that as high lead concentrations are approached, agreement becomes very bad. The reason for this bad agreement is assigned at the moment to the failure of the force-constant analysis used to calculate $F(\omega)$.²⁹ As the electron concentration is increased, the electron-phonon coupling becomes stronger, longer-range forces become significant, and the dispersion curves are correspondingly more structured. In pure lead, for example, strong Kohn anomalies are observed. These highly structured dispersion curves become increasingly difficult to fit with a finite number of force constants, and the model becomes physically unrealistic. In lead, although the measured symmetry-direction dispersion curves are fitted fairly well, and the critical points generated by these Van Hove singularities agree with the inversions of McMillan and Rowell, the model incorrectly predicts off-symmetry critical points. Recently, Stedman *et al.*³³ have arrived at the same conclusion by experimentally sampling throughout the Brillouin zone, and were able to produce an $F(\omega)$ in better agreement with the tunneling work. The disagreements in the strengths of particularly the longitudinal peaks are not well understood as yet. In

pure lead, for example, although the critical points do not agree, the strengths of these peaks do. However, upon alloying there appears a smearing of the narrow longitudinal peak. A similar effect may be observed in the work of Adler *et al.*,³⁴ where this occurs whether lead is alloyed with Bi or Tl.

In the calculation of $\alpha^2(\omega)F(\omega)$ from a Born-von Kármán model, no provision is made for the disordered nature of the alloy, and the simple assumption is made that every lattice site is identical, consisting of an "average" ion. Disordered systems may be expected to produce lifetime broadening due to random differences in the forces between pairs of ions. This broadening will lead to a smearing of the frequency distribution in the alloy system not present in the pure material. While we have at present no quantitative estimate of this effect, there is experimental and theoretical evidence that it is not at all unreasonable that the higher-energy longitudinal modes might be more affected.³⁵

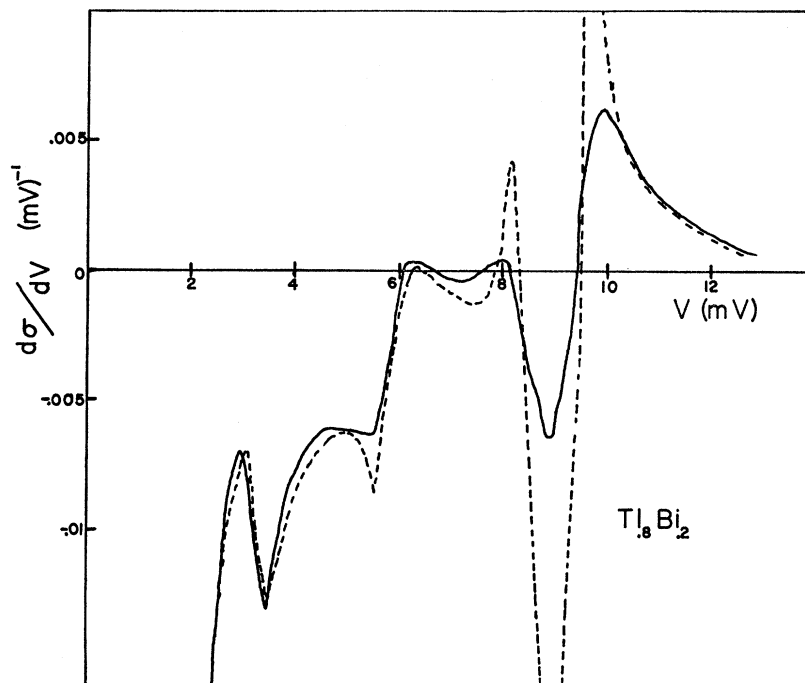
VI. CONCLUSIONS

With a reliable knowledge of the pseudopotential form factor for scattering from and to points on the Fermi surface, and with accurate information about the lattice dynamics of the material under question, it is possible to predict reliably the superconducting parameters of a material. Through a determination of the product func-

³⁴ J. G. Adler, J. E. Jackson, and T. A. Will, Phys. Letters **24A**, 407 (1967).

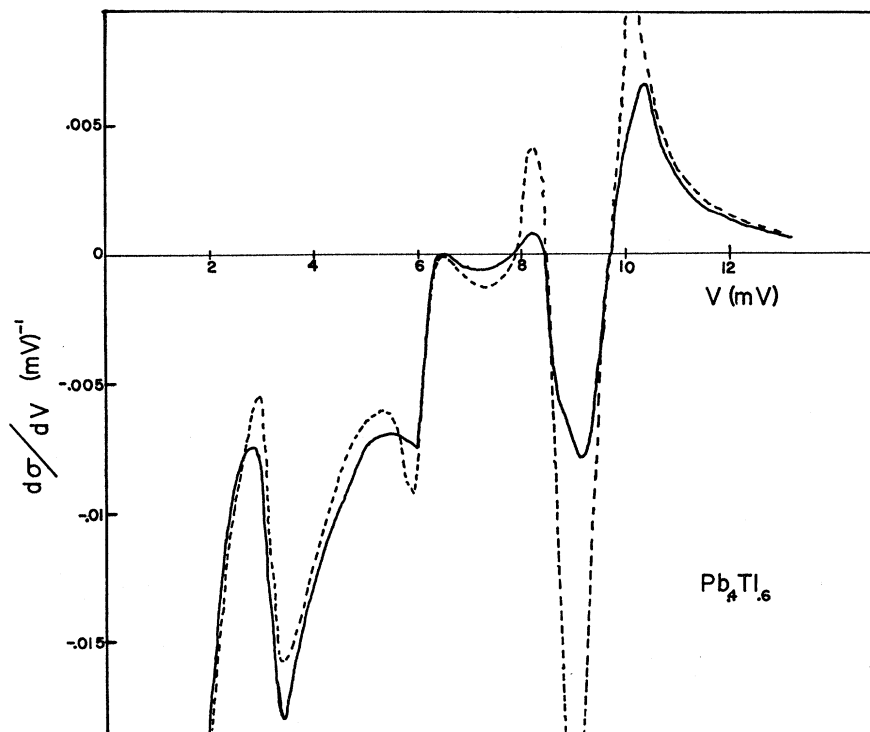
³⁵ B. N. Brockhouse, in *Phonons in Perfect Lattices and in Lattices with Point Imperfections*, edited by R. W. H. Stevenson (Oliver and Boyd, Edinburgh, 1966).

³³ R. Stedman, L. Almquist, and G. Nilson, Phys. Rev. **162**, 549 (1967).



(a)

FIG. 7. Comparison of calculated (dashed line) and experimental (solid line) $d\sigma/dV$ versus V plots for junctions of (a) Al-I-Tl_{0.8}Bi_{0.2} and (b) Al-I-Pb_{0.4}Tl_{0.6} at 1.1°K.



(b)

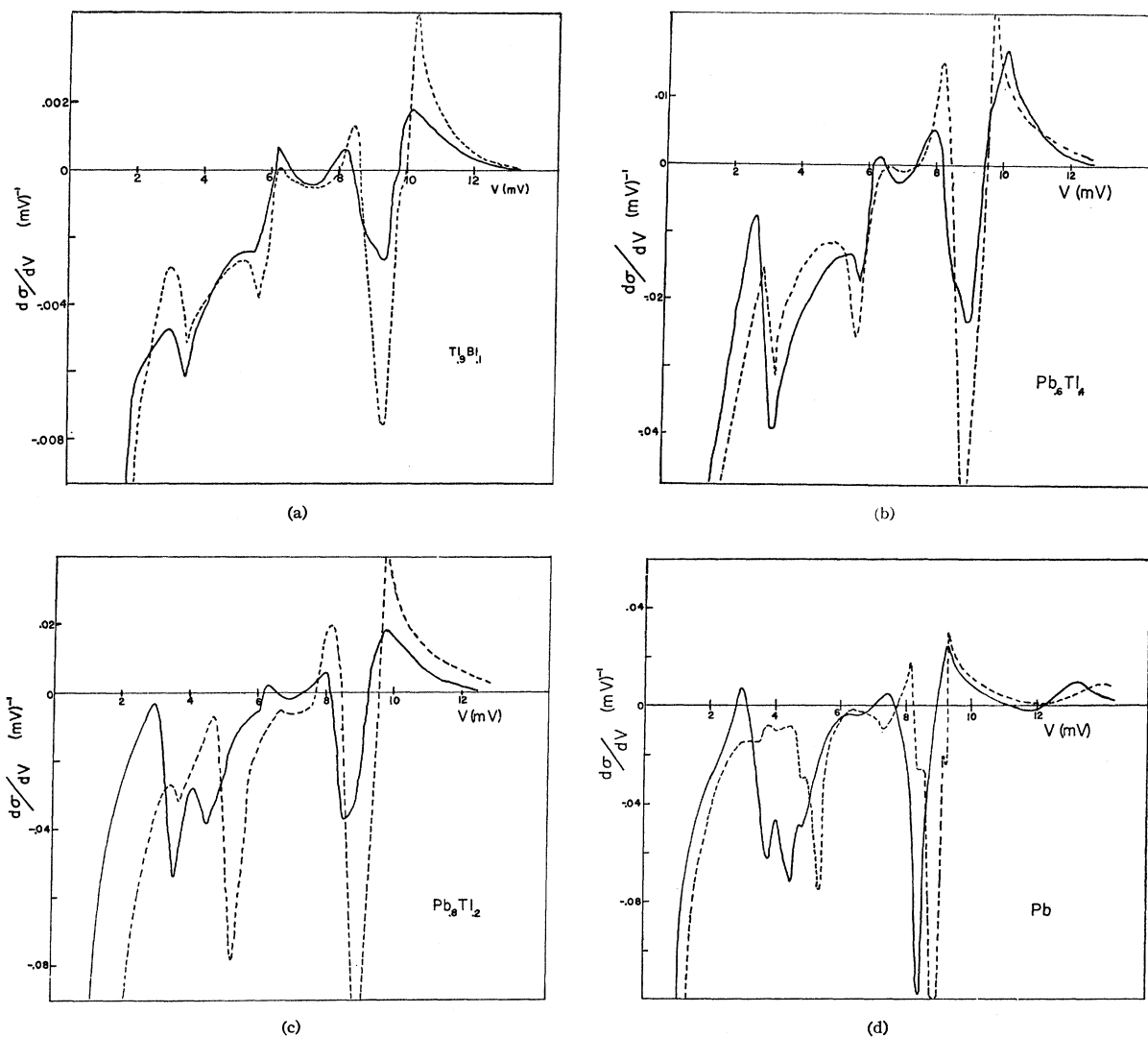


FIG. 8. Comparison of calculated (dashed line) and experimental (solid line) $d\sigma/dV$ versus V plots for junctions of (a) Al-I-Tl_{0.9}Bi_{0.1}, (b) Al-I-Pb_{0.6}Tl_{0.4}, (c) Al-I-Pb_{0.8}Tl_{0.2}, and (d) Al-I-Pb at 1.1°K.

tion $\alpha^2(\omega)F(\omega)$ and a solution of the energy-gap equations, the zero-temperature superconducting energy gaps $\Delta(\Delta_0)$ can be determined and are found to agree very well with electron tunneling experimental determinations of the same quantity.

In addition, it is shown that reasonable agreement should be expected in determining the phonon-spectrum critical points by neutron scattering experiments and tunneling. Questionable agreement in the past is attributed to the nonconvergence of the force-constant model used to analyze the measured dispersion relations.

Good agreement in the strengths of the tunneling peaks reflecting these singularities is not achieved, but it is thought this is possibly due to the alloy nature of the material considered.

ACKNOWLEDGMENTS

The authors are grateful to B. N. Brockhouse, S. C. Ng, and E. D. Hallman for making their data available and for many valuable discussions. We also thank J. M. Rowell for helpful suggestions and comments regarding the manuscript.